

Predicting trends in atmospheric CO₂ across the Mid-Pleistocene Transition using existing climate archives

Jordan R.W. Martin¹, Joel Pedro^{2,3}, Tessa R. Vance³

¹Institute for Marine and Antarctic Studies, University of Tasmania, Hobart, 7004, Australia

²Australian Antarctic Division, Kingston, 7050, Australia

³Australian Antarctic Program Partnership, Institute for Marine and Antarctic Studies, University of Tasmania, Hobart, 7004, Australia

Correspondence to: Jordan R.W. Martin (jrmartin@utas.edu.au)

Abstract

During the Mid-Pleistocene Transition (MPT), ca. 1200–800 thousand years ago (kya), the Earth's glacial cycles changed from 41 kyr to 100 kyr periodicity. The emergence of this longer ice-age periodicity was accompanied by higher global ice volume in glacial periods and lower global ice volume in interglacial periods. Since there is no known change in external orbital forcing across the MPT, it is generally agreed that the cause of this transition is internal to the earth system. Resolving the climate, carbon cycle and cryosphere processes responsible for the MPT remains a major challenge in earth and palaeoclimate science. To address this challenge, the international ice core community has prioritised recovery of an ice core record spanning the MPT interval.

Here we present results from a simple generalised least squares (GLS) model that predicts atmospheric CO₂ out to 1.8 Myr. Our prediction utilises existing records of atmospheric carbon dioxide (CO₂) from Antarctic ice cores spanning the past 800 kyr along with the existing LR04 benthic $\delta^{18}\text{O}_{\text{calcite}}$ stack (Lisiecki & Raymo, 2005; hereafter 'benthic $\delta^{18}\text{O}$ stack') from marine sediment cores. Our predictions assume that the relationship between CO₂ and benthic $\delta^{18}\text{O}$ over the past 800 thousand years can be extended over the last one and a half million years. The implicit null hypothesis is that there has been no fundamental change in feedbacks between atmospheric CO₂ and the climate parameters represented by benthic $\delta^{18}\text{O}$, global ice volume and ocean temperature.

We test the GLS-model predicted CO₂ concentrations against observed blue ice CO₂ concentrations, $\delta^{11}\text{B}$ -based CO₂ reconstructions from marine sediment cores and $\delta^{13}\text{C}$ of leaf-wax based CO₂ reconstructions (Higgins *et al.*, Yan *et al.*, 2019 and Yamamoto *et al.*, 2022). We show that there is not clear evidence from the existing blue ice or proxy CO₂ data to reject our predictions nor our associated null-hypothesis. A definitive test and/or rejection of the null hypothesis may be provided following recovery and analysis of continuous oldest ice core records from Antarctica, which are still several years away. The record presented here should provide a useful comparison for the oldest ice core records and opportunity to provide further constraints on the processes involved in the MPT.

37 **1 Introduction**

38 Ice core records from Antarctica provide comprehensive and continuous records of many climate parameters
39 over the last 800 thousand years, e.g. from the Vostok (Petit *et al.*, 1999) and European Project for Ice Coring in
40 Antarctica's Dome-C (EDC) ice cores (Jouzel *et al.*, 2007). One of the major challenges in climate science lies
41 beyond the current threshold of the ice core record. The Mid-Pleistocene Transition (MPT) spans from ca.
42 1200–800 thousand years ago (kya) (Chalk *et al.*, 2017) and is characterised by a change from regularly paced
43 40 thousand year (kyr) glacial cycles with thinner glacial ice sheets to quasi-periodic 100 kyr glacial cycles in
44 which ice sheets are more persistent and thicker (Clark *et al.*, 2006, Chalk *et al.*, 2017). To resolve the forcings
45 and feedbacks involved in this transition, multiple nations are targeting recovery of continuous ice cores
46 spanning the MPT under the framework of the International Partnerships in Ice Core Science (IPICS) oldest ice
47 core challenge (IPICS, 2020).

48

49 The purpose of the current study is to make a simple prediction of atmospheric CO₂ across the MPT. Cross-
50 comparison of our and other predicted CO₂ records against observed MPT CO₂ data will aid in testing
51 competing hypotheses on the cause of the transition, in particular the role of carbon cycle changes.

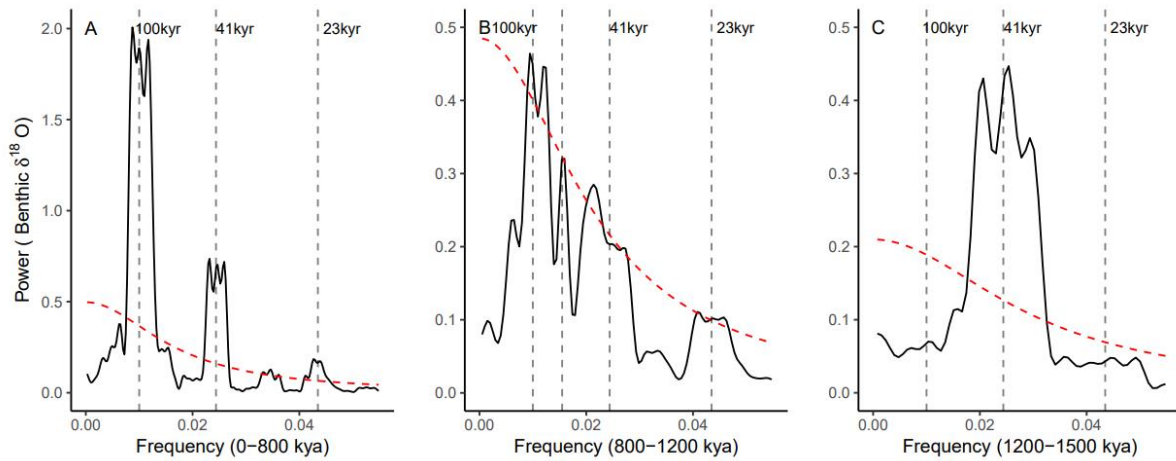
52

53 The MPT occurred in the absence of any changes to orbital insolation forcing; **therefore, the mechanisms** behind
54 the MPT must be internal to the earth system (Raymo, 1997; Ruddiman *et al.*, 1989). Multiple hypotheses have
55 been put forward to explain the transition. **A common element in many of these is internal** climate/earth system
56 changes which allow for the development of thicker, more extensive ice sheets that could endure insolation
57 peaks corresponding to the 23 kyr precession and 41 kyr obliquity cycles, i.e., an increase in the threshold for
58 deglaciation and altered sensitivity to orbital forcings (McClymont *et al.*, 2013; Tzedakis *et al.*, 2017). Indeed,
59 the skipped obliquity cycle hypothesis, proposes that 100 kyr signal seen in spectral analysis of the post-MPT
60 benthic $\delta^{18}\text{O}$ stack (e.g. Fig 1A) may be comprised of alternating 80 and 120-kyr signals, i.e. in which the
61 intervening obliquity cycles are skipped. Among the prominent hypotheses to explain an increased threshold for
62 deglaciation are the following three.

- 63 1) A long- term decrease in radiative forcing due to a secular reduction in atmospheric CO₂ across the
64 transition (e.g. Berger *et al.*, Hönisch *et al.*, 2009; 1999, Raymo *et al.*, 1988). According to this view,
65 reduced radiative forcing drives the formation of larger and more stable ice sheets.
- 66 2) Progressive removal of sub-glacial regolith during the 41 kyr glacial cycles. Clark & Pollard (1998)
67 proposed that ice sheet basal sliding prior to the MPT was enhanced by the presence of a low-friction
68 sedimentary regolith layer between the Laurentide ice sheet and the crystalline bedrock. According to
69 this view, progressive removal of this sedimentary layer then favoured the development of larger and
70 more persistent post-MPT ice sheets.
- 71 3) Phase-locking of the Northern and Southern Hemisphere ice sheets. In frequency spectra of the global
72 marine benthic $\delta^{18}\text{O}$ record (Fig. 1) there is no evidence of the precession (23 kyr) component of
73 northern hemisphere insolation prior to the MPT; the spectra is dominated by the obliquity (41 kyr)
74 component (Fig. 1C). Emergence of significant precession and 100 kyr signals occurs across the MPT
75 (Fig. 1B), and all three components are clearly present after the MPT (Fig. 1A). Raymo *et al.* (2006)
76 suggested that precession-paced changes in northern and southern hemisphere ice volumes may have

77 occurred prior to the MPT, but are cancelled due to out-of-phase ice volume changes between the two
 78 hemispheres. (Raymo & Huybers, 2008). According to this view, during the MPT the precession-paced
 79 changes fall into phase between the two hemispheres, such that the precession signal emerges (Raymo
 80 *et al.*, 2006). In this view the global synchronisation of ice volume drives the formation of larger and
 81 more stable ice sheets.

82
 83 These hypotheses are not mutually exclusive. For a recent review on the cause of the MPT see Berends *et al.*
 84 (2021a).



86
 87
 88 **Figure 1: Thomson Multi-taper Method (MTM) spectral analysis representing relative power of signal periodicity for:**
 89 **A) Benthic $\delta^{18}\text{O}$ stack after (0–800 kya) the Mid-Pleistocene Transition (MPT); B) Benthic $\delta^{18}\text{O}$ across the MPT (800–**
 90 **1200 kya); C) Benthic $\delta^{18}\text{O}$ prior to the onset of the MPT (1200 kya–1500 kya). Each with a robust AR (1) 95 %**
 91 **Confidence interval (red dashed line). Benthic $\delta^{18}\text{O}$ stack data from Lisiecki and Raymo (2005).**

92
 93 **For a long-term decrease in radiative forcing by atmospheric CO_2 to be the cause of the MPT, the reduction in**
 94 **CO_2 might be expected in both glacial and interglacial stages** (Chalk *et al.*, 2017). However, low resolution
 95 boron-isotope-based CO_2 reconstructions by Hönisch *et al.*, (2009), and Chalk *et al.*, (2017) suggest that glacial-
 96 stage CO_2 drawdown occurred over the MPT in the absence of interglacial CO_2 drawdown. Glacial-stage CO_2
 97 draw-down across the MPT may be a positive climate-carbon cycle feedback to changes in ice sheet dynamics,
 98 including CO_2 drawdown by enhanced iron fertilisation of the Southern Ocean in response to exposed
 99 continental shelves due to lower sea level, as well as planetary drying associated with colder climate conditions
 100 (Chalk *et al.*, 2017). Colder glacial temperatures that enhance the solubility of CO_2 in the oceans, and reduced
 101 abyssal ocean ventilation has also been implicated in enhanced glacial-stage ocean storage of CO_2 (McClymont
 102 *et al.*, 2013; Hasenfratz *et al.*, 2019).

103
 104 Testing of hypotheses on the cause of the MPT is currently limited by the lack of a continuous ice core that
 105 spans its duration. The International Partnership in Ice Core Sciences (IPICS) has nominated recovery of such a
 106 record as a key priority in ice core research (IPICS, 2020). Multiple national and international projects have
 107 commenced, or are soon to commence, drilling for ‘oldest ice’ (see e.g. Shugi, 2022). In this project, we take

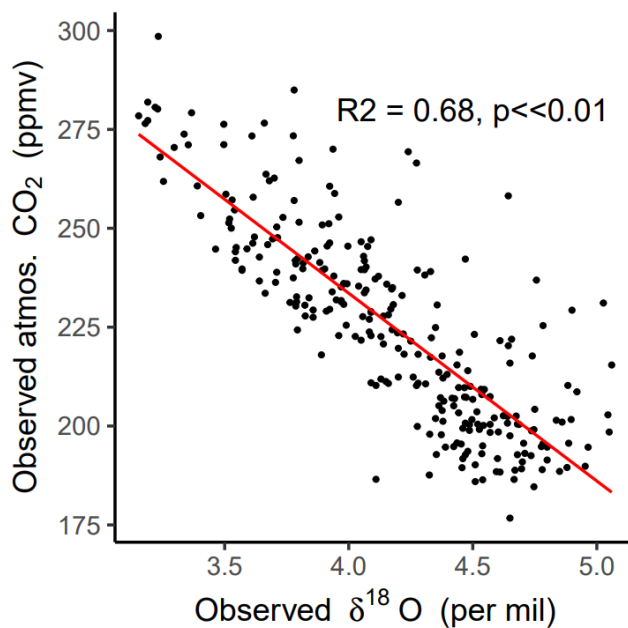
108 inspiration from the “EPICA Challenge” in which the paleoclimate and modeling community was challenged to
109 predict the global atmospheric carbon dioxide and methane concentrations from 800–400 kya based on the
110 existing 400 kyr Vostok ice core record (Wolff *et al.*, 2004). Here, we use a generalised least squares (GLS)
111 model trained on continuous climate archives to predict a CO₂ record out 1.8 Mya. We utilise two primary data
112 sets for the GLS model: the existing 800 kyr ice core composite record of atmospheric CO₂ (Bereiter *et al.*,
113 2015) and the LR04 benthic stack of 57 globally-distributed records of the ¹⁸O to ¹⁶O ratio of fossil benthic
114 foraminifera calcite (hereafter referred to as the LR04 δ¹⁸O benthic stack). The δ¹⁸O ratios in the LR04 benthic
115 stack are governed primarily by deep ocean temperature and global ice volume at the time the foraminifera
116 lived, with higher values indicating both increased ice volume and a colder climate. The relationship between
117 the ice volume and ocean temperature components contributing to the δ¹⁸O benthic stack are not linear.
118 Separating the two signals remains challenging and has been attempted elsewhere using a range of approaches
119 from comparison with paired deep ocean temperature proxies (Elderfield *et al.*, 2012), inverse modelling
120 (Berends *et al.*, 2021b) and spectral analysis (e.g. Huybers and Wunsch, 2009).

121
122 Fig. 2 shows a scatter-plot of the LR04 δ¹⁸O benthic stack versus observed ice core CO₂ over the past 800 kyr.
123 Both data sets are binned to equivalent 3-kyr time steps (Methods). The Pearson’s correlation coefficient (r)
124 between the data sets is -0.82 (p < 0.05) indicating that ~68% of the variance in observed CO₂ is shared with the
125 LR04 δ¹⁸O benthic stack. This strong relationship provides an initial rationale for using the LR04 δ¹⁸O benthic
126 stack as an input parameter to predict CO₂ beyond 800 kyr. Mechanistically, multiple processes are expected to
127 contribute to the shared variance. A first order factor is the dependency of CO₂ solubility on ocean temperature
128 (e.g. Millero, 1995). From the simple solubility perspective, colder climate states with increased ice volume and
129 colder ocean temperatures will drive increased ocean uptake of CO₂ (Berends *et al.*, 2021a). However, the
130 solubility effect only accounts for a portion of observed glacial CO₂ drawdown (Archer *et al.*, 2000). Multiple
131 additional contributors to the shared variance are proposed in the literature. These include (not exhaustively),
132 direct radiative forcing of ice volume changes by CO₂ (e.g. Shackleton *et al.*, 1985); the impact of ice
133 volume/sea level changes on atmospheric CO₂ via ocean productivity and carbonate chemistry changes (e.g.
134 Broecker, 1982; Archer *et al.*, 2000; Ushie and Matsumoto, 2012); CO₂ drawdown during periods of high ice
135 volume by increased iron fertilisation (e.g. Röthlisberger *et al.*, 2004; Martinez-Garcia *et al.*, 2014) and
136 enhanced sea ice extent during periods of high ice volume capping the ventilation of CO₂ from the ocean
137 interior at high latitudes (Stephens and Keeling, 2000).

138
139 A quantitative separation and attribution of the processes linking global ice volume, ocean temperature and
140 atmospheric CO₂ on millennial to orbital timescales is not currently available (e.g. Archer *et al.*, 2000; Sigman
141 *et al.*, 2010; Gottschalk *et al.*, 2019) and will not be attempted here. Rather, we make the simple assumption that
142 the relationships between the LR04 benthic δ¹⁸O stack and CO₂ can be extended beyond 800 kya and use
143 generalised least squares (GLS) regression modelling between benthic δ¹⁸O and CO₂ to make a prediction of
144 CO₂ spanning 800–1500 kya. The deliberately simple implicit assumption, and null hypothesis, is that there is
145 no change to the feedback processes linking benthic δ¹⁸O and CO₂ before and after the MPT.

146

147 This approach differs to previous more complex model studies that have attempted to reconstruct CO₂ using the
 148 LR04 benthic δ¹⁸O stack as an input variable (van de Wal, 2011; Stap *et al.*, 2016, Berends *et al.*, 2021b). The
 149 latter studies use an inverse forward modelling approach, in which climate and ice sheet models of various
 150 complexities are used to capture physical relations between CO₂, global temperature and ice volume. For
 151 example, in Berends *et al.*, 2021b the offset between modelled and observed benthic δ¹⁸O is used to calculate a
 152 value for atmospheric CO₂ that is iterated back to the inverse model. The CO₂ record which minimises the
 153 difference between the modelled and observed benthic stack is then taken as an estimate of how atmospheric
 154 CO₂ may have evolved to force coupled climate, deep ocean temperature and land ice volume changes that
 155 reproduce the observed benthic δ¹⁸O signal. Accuracy of the reconstructions in the inverse modelling approach
 156 depends on the ability of the climate and ice sheet models used to capture the correct climate dynamics across
 157 the MPT. Our GLS method is a simpler statistical approach, designed with the specific null hypothesis in mind,
 158 that does not attempt to simulate the physics linking benthic δ¹⁸O signal, land ice volume, global temperature
 159 and CO₂. A range of approaches to reconstructing CO₂ have been called for and are of value in the context of
 160 forthcoming continuous ice core records across the MPT from oldest ice projects currently underway in
 161 Antarctica [IPICS 2020].
 162



163 **Figure 2: Scatter plot of the composite observed atmospheric CO₂ record (Bereiter *et al.*, 2015) against**
 164 **the LR04 benthic stack of marine δ¹⁸O records (Lisiecki & Raymo, 2005). Red line is a linear line of best**
 165 **fit ($R^2 = 0.68$; $p < 0.05$).**

166
 167
 168 To test our null hypothesis, in advance of the recovery of a continuous ice core, we compare our predicted CO₂
 169 record to two sets of low-resolution ice core data that exist outside the current 800 kyr observed CO₂. These data
 170 come from direct CO₂ measurements from ancient “blue ice” from the Allan Hills in East Antarctica (hereafter
 171 referred to as BI-CO₂) from ca. 1 Mya (Higgins *et al.*, 2015) and 1.5 Mya (Yan *et al.*, 2022). We use the term
 172 blue ice to describe deep, ancient glacial ice that has been brought nearer to the surface of an ice sheet by ice

173 flow. Blue ice is sampled by cutting trenches or shallow drilling of up to several hundred meters (e.g. Higgins *et*
174 *al.*, 2015). The vertical migration of blue ice is associated with high deformation making the ice samples
175 stratigraphically complex and hard to date (Higgins *et al.*, 2015). As a result, blue ice records alone do not
176 provide a continuous CO₂ record across the MPT. In the Discussion, we also compare our predicted record to
177 existing proxy-CO₂ reconstructions from boron-isotope analysis of benthic foraminifera in marine sediment
178 records (Chalk, *et al.*, 2017; Dyez *et al.*, 2018; Guillermic *et al.*, 2022), leaf wax δ¹³C carbon isotope ratios
179 (Yamamoto *et al.*, 2022) and predictions from previous models of various complexities (van de Wal *et al.*, 2011;
180 Willeit *et al.* 2019; Berends *et al.* 2021b). We conclude with discussion of the implications of our results and
181 data-comparisons for the understanding MPT dynamics.

182

183

184 **2 Methods**

185

186 We use a generalised least squares (GLS) model with an auto-regressive (AR) factor 1 to predict atmospheric CO₂
187 from the LR04 benthic δ¹⁸O stack (Fig. 3A and B). We use GLS because the assumptions of ordinary least squares
188 (OLS) are violated by the presence of autocorrelation and heteroskedasticity in the regression errors. We selected
189 the AR(1) correlation factor as it yielded the lowest Akaike information criterion (AIC) value from a test of
190 multiple correlation factors. The AR(1) process assumes and accounts for dependence of error at a given point in
191 time on the previous error term. In practise this makes the model assumptions more realistic and improves
192 parameter estimation where, as in the climate system, observations are dependent on past values.

193

194 To obtain common time steps and resolution between the predictor (LR04 benthic δ¹⁸O stack) and response
195 (CO₂) variables, we re-grid the LR04 benthic stack and Bereiter *et al.*, (2015) CO₂ data into time bins with a
196 resolution of 3-kyr. The GLS regression model was then applied over the 0 – 800 kyr range of the predictor and
197 response variables as follows:

198

$$199 \quad CO_2 = - 33.37 \times \delta^{18}O + 365.15, \text{ autoregressive (AR) factor: 1}$$

200

201 Based on the regression model, the δ¹⁸O values of the LR04 Benthic Stack from 800 – 1500 kya were used to
202 predict CO₂ concentration over this range (hereafter referred to as PRED-CO₂). To gauge the GLS model
203 stability we took a bootstrap approach, selecting a random 50% subset of our data (with replacement) and re-
204 running the model 1000 times to determine 95% confidence intervals for the predictions. While the GLS method
205 itself addresses autocorrelation, the bootstrap method introduces variability such that each iteration of the model
206 has different combinations of the original data points (including repeated ones), this variability helps in
207 assessing the robustness and sensitivity of the model e.g. to variable data and dating uncertainty.

208

209 Uncertainties in the independent age scales of both the LR04 stack and the compiled CO₂ record are inherited by
210 our GLS model and its predictions. The LR04 stack includes 57 globally-distributed benthic δ¹⁸O sediment core
211 records. The age models for these cores are constructed by alignment of their δ¹⁸O signals, followed by tuning
212 of the stack to a simple ice model based on 21 June insolation at 65°N in a way which maintains relatively
213 stable global mean sedimentation rates. The age models for these cores are independently constructed from the

214 ~~average sedimentation rates of each core, assuming global sedimentation rates have remained relatively stable,~~
215 ~~and with tuning to a simple ice model based on 21 June insolation at 65°N~~ (Lisiecki & Raymo, 2005). The
216 authors estimate uncertainty of 6 kyr from 1.5 – 1.0 Mya and 4 kyr from 1 – 0 Mya (Lisiecki & Raymo, 2005).
217 The observed CO₂ composite ice core record for the past 800 kya (Bereiter *et al.*, 2015) uses six independent
218 dating methods for various core locations both spatially across Antarctica, and stratigraphically for different
219 sections of the same core. The age uncertainty in the gas timescale has a median over the 0 – 800 kya interval of
220 2 kyr, but individual uncertainties can reach up to 5 kyr (Veres *et al.* 2013; Bazin *et al.*, 2013). The relative age
221 uncertainties between these input variables may diminish the regression or in some instances lead to spurious
222 correlation. However, we expect any such effects are minor on the basis that our predictions show little
223 sensitivity (~~median, 2 σ , 5.78 ppm~~) to the bootstrap analysis: with a median 2 σ error of 5.8 ppm from 0 to 1.8
224 Mya (see Fig. 3B, C and Discussion).

225

226 3 Results

227 Fig. 3B shows the time series of our LR04 benthic $\delta^{18}\text{O}$ stack-based GLS model predictions of atmospheric CO₂
228 (PRED-CO₂) over the past 800 kyr, in comparison to the observed ice core CO₂ record from Bereiter *et al.*,
229 (2015). The correlation coefficient (R^2) between the predicted and observed records is 0.68 ($p \ll 0.01$). Our
230 PRED-CO₂ record out to 1.8 Mya with shaded 95% CIs from the bootstrap analysis is also shown, overlain with
231 observed Allan Hills blue ice CO₂ (BI-CO₂) datasets of age 1000 ± 89 kya (Higgins *et al.*, 2015) and $1.5 \text{ Mya} \pm$
232 213 kyr (Yan *et al.*, 2022).

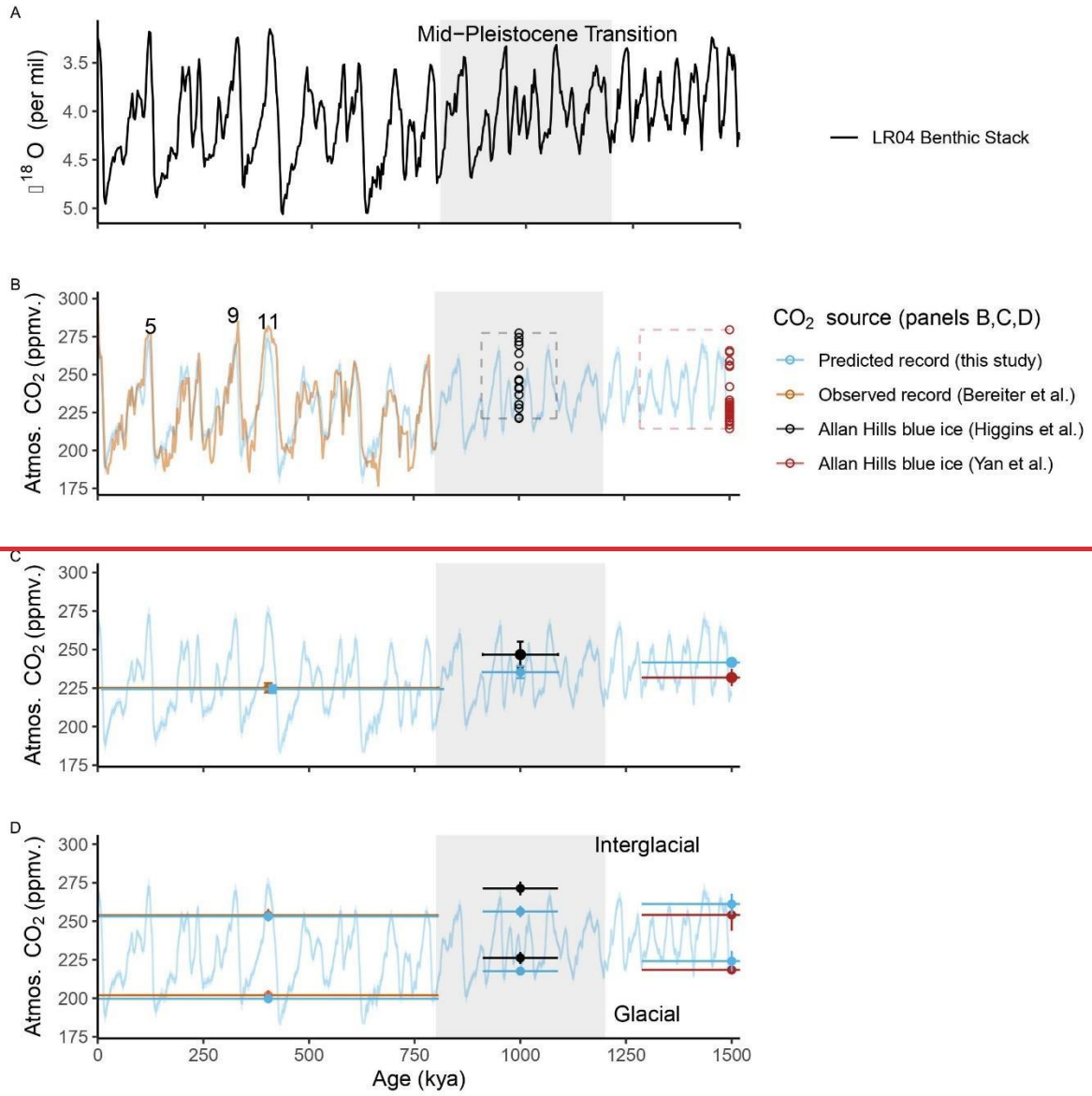
233

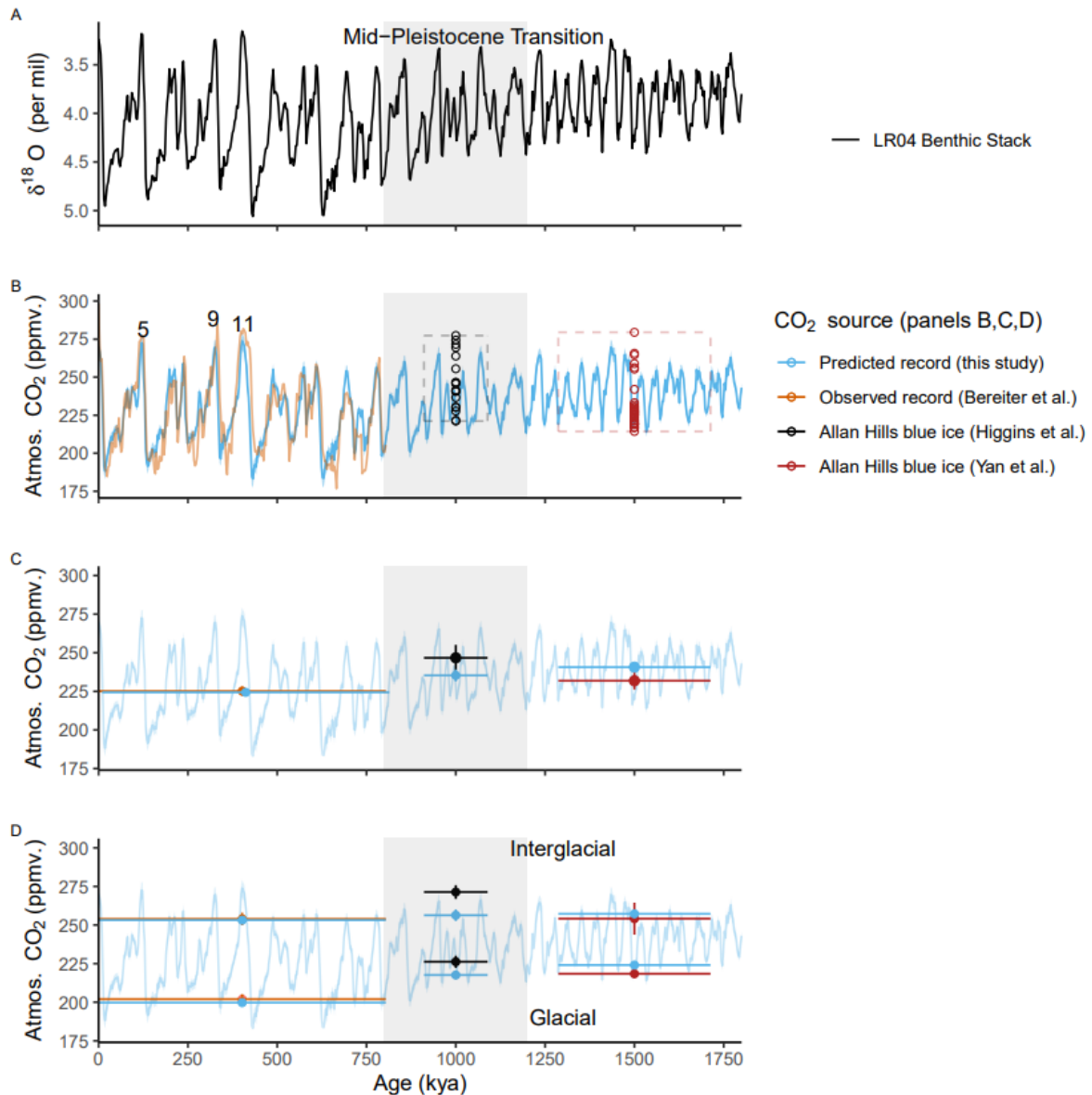
234 We evaluate the PRED-CO₂ record against the observed CO₂ data according to criteria of mean concentrations
235 across the common intervals, and mean concentrations in the glacial and interglacial subsets of the data. First,
236 the mean CO₂ concentration over the common intervals (Fig 3C). From 0 – 800 kya the mean concentration in
237 observed (Bereiter *et al.*, 2015) and PRED-CO₂ data are in close agreement (225.2 ± 3.03 ppm versus the
238 predicted 225.21 ± 2.5 ppm respectively; uncertainties are 95% confidence intervals, i.e. 1.96σ). In the $1000 \pm$
239 89 kya interval (i.e. averaged across the age uncertainty of the Higgins *et al.* (2015) blue ice data) the BI-CO₂
240 concentration is ~ 11 ppm higher than PRED-CO₂ (246.7 ± 8.4 ppm versus the predicted 235.35 ± 3.9 ppm), this
241 difference is not significant at the 95% confidence level. For the $1.5 \text{ Mya} \pm 213$ kyr interval, the mean BI-CO₂
242 concentration is ~ 9 ppm lower than PRED-CO₂ (231.9 ± 5.6 ppm versus the predicted 240.7 ± 2.1 ppm), which
243 is marginally significant at the 95% level. Comparisons of mean levels across intervals spanning multiple glacial
244 and interglacial cycles may be biased if (as is likely) the blue ice data is not sampling glacial and interglacial
245 values with the same uniformity as a continuous record.

246

247 To address this, we define the glacial and interglacial thresholds of PRED-CO₂ to be respectively the lower and
248 upper 25th percentiles of the LR04 $\delta^{18}\text{O}$ predictor variable (following Chalk *et al.*, 2017). Filtering the observed
249 (Bereiter *et al.*, 2015) CO₂ record and our predicted CO₂ record according to these definitions we find a very
250 close match for glacial (202.0 ± 3.2 versus the predicted 199.7 ± 1.6 ppm) and interglacial intervals (253.9 ± 4.1
251 ppm versus the predicted 253.1 ± 2.3 ppm), over the past 800 kya (see Fig. 3D for these comparisons). For blue
252 ice (BI-CO₂) data, a corresponding LR04 isotope signal could not be confidently applied to the measured CO₂
253 concentration due to the uncertainties associated with blue ice dating-; therefore, we defined the glacial and

254 interglacial thresholds of blue ice data according to the top (interglacial) and bottom (glacial) 25th percentiles of
255 actual CO₂. Applying this to the 1000 ± 89 kya interval finds that observed BI-CO₂ data is ~9 ppm higher than
256 PRED-CO₂ during the glacial stages (226.2 ± 4.0 ppm versus the predicted 217.6 ± 2.3 ppm) and ~15 ppm
257 higher than PRED-CO₂ during the interglacial stages (271.3 ± 4.5 versus the predicted 256.3 ± 3.8 ppm). These
258 differences are significant with respect to the constrained uncertainties. ~~However, during the 1.5 Mya ± 213 kyr~~
259 ~~interval, the mean BI-CO₂ concentration is not significantly different to PRED-CO₂ in either glacial (217.6 ± 2.3~~
260 ~~versus the predicted 224.2 ± 6.6 ppm) or interglacial stages (256.3 ± 3.8 versus the predicted 261.1 ± 6.3 ppm).~~
261 ~~These comparisons, particularly the agreement at 1.5 Myr, indicate that PRED-CO₂ is not drifting systematically~~
262 ~~away from the existing observed BI-CO₂ data. In our view the disagreement at 1.0 Myr, where BI-CO₂ is~~
263 ~~elevated with respect to PRED-CO₂, does not give sufficient cause to reject the GLS model, it could of course~~
264 ~~be a failing in the model and/or could be due to potential biases in the blue ice data, for example elevated CO₂~~
265 ~~concentrations due to in situ CO₂ production in blue ice (see Discussion).~~ During the 1.5 Mya ± 213 kyr
266 interval, the mean BI-CO₂ concentration did not show any significant difference to PRED-CO₂ in interglacial
267 stages (254.1 ± 10.3 versus the predicted 257.2 ± 1.7 ppm. During glacial stages there is a small 2.9 ppm
268 difference between the upper estimate of BI-CO₂ and the lower estimate of PRED-CO₂ (218.4 ± 1.3 and 224 ±
269 1.4 ppm respectively, see Fig 3D). In our view these results, notwithstanding the 2.9 ppm difference at 1.5 Mya,
270 do not give sufficient cause to reject the GLS model. Furthermore, the comparison indicates that PRED-CO₂ is
271 not drifting systematically away from the existing observed BI-CO₂ data (Fig 3D). The differences could of
272 course be a failing in the model, potential biases in the blue ice data, dating uncertainty and/or other
273 unconstrained uncertainties (see Discussion for blue ice caveats).





275

276 **Figure 3: A) The LR04 Benthic Stack of 57 globally distributed $\delta^{18}\text{O}$ records (Lisiecki & Raymo, 2005).**

277 **B) Comparison of our PRED-CO₂ (ppm) record to the current continuous composite record (0–800 kya);**

278 **and to direct CO₂ measurements from Allan Hills blue ice cores (BI-CO₂) ca. 1 Mya (± 89 kyr) (Higgins *et***

279 ***al.*, 2015) and ca. 1.5 Mya (± 213 kyr) (Yan *et al.*, 2022). Age uncertainty boundaries for the BI-CO₂ data**

280 **are represented by dashed box boundaries. Marine isotope stages 5, 9, and 11 are numbered on the plot**

281 **according to Lisiecki & Raymo (2005). Blue shading around PRED-CO₂ is the 95% CI from bootstrap**

282 **analysis. C) Mean concentrations of the PRED-CO₂ and observed composite CO₂ records over the range of the observed composite record (offset for clarity), and the mean concentrations of the PRED-CO₂ and**

283 **BI-CO₂ data at 1 Mya and again at 1.5 Mya averaged over the age uncertainty range of each BI-CO₂ data**

284 **set. D) As for C) however filtered by the upper and lower 25th and 75th percentiles to estimate glacial and**

285 **interglacial periods.**

286 **interglacial periods.**

287

288 We now consider long-term trends in interglacial and (separately) glacial CO₂ levels across the past 1.8 Myr in

289 PRED-CO₂ and in the existing ice core CO₂ data. For PRED-CO₂ there is no significant difference between CO₂

290 concentrations in the interglacial stages of the $1.5 \text{ Mya} \pm 213 \text{ kya}$, $1000 \pm 89 \text{ kya}$ and $0\text{--}800 \text{ kya}$ windows (Fig 4
291 D, blue bars). In the ice core observations, interglacial levels at 1.5 Mya in BI-CO₂ are also within the
292 uncertainties of those in the $0\text{--}800 \text{ kya}$ interval. Notably, the BI-CO₂ concentrations in the $1000 \pm 89 \text{ kya}$
293 interval appear elevated with respect to the $0\text{--}800 \text{ kyr}$ and $1.5 \text{ Mya} \pm 213 \text{ kya}$ intervals, however this elevated
294 (ca. 271 ppm) level is consistent with the observed interglacial CO₂ concentration during interglacials 5, 9 and
295 11 (Fig 3B). Overall, there is no indication in the observed ice core CO₂ data or in PRED-CO₂ for a long-term
296 trend in *interglacial* CO₂ levels across the past 1.8 Myr.

297

298 In comparison, there are significant declines in glacial CO₂ levels across the MPT in PRED-CO₂ and the
299 observed ice core data. For PRED-CO₂, glacial CO₂ concentrations are not significantly different during the 1.5
300 $\text{Mya} \pm 213 \text{ kya}$ and $1000 \pm 89 \text{ kya}$ windows. However, across the MPT, PRED-CO₂ glacial concentrations drop
301 by $\sim 18 \text{ ppm}$ (Fig 3D). This pattern is consistent with similar to the observed BI-CO₂ data, where glacial CO₂
302 levels show no decline are also not significantly different between the $1.5 \text{ Mya} \pm 213 \text{ kya}$ and $1000 \pm 89 \text{ kya}$
303 windows (indeed there is a marginal increase from 2187.46 ± 12.3 to $226.2 \pm 4.0 \text{ ppm}$, respectively), before
304 falling by 24 ppm to the $0\text{--}800 \text{ kyr}$ observed glacial mean of $202.0 \pm 3.2 \text{ ppm}$ (Fig 3D). Glacial-stage draw-
305 down of CO₂ across the MPT in the absence of interglacial draw-down is consistent with previous observations
306 based on the boron-isotope-based CO₂ reconstructions (e.g., Chalk *et al.*, 2017; Hönisch *et al.*, 2009 and see
307 Discussion). In the following section we also compare PRED-CO₂ data to boron-isotope-based and other CO₂
308 proxy records covering the 0 to 1.8 Myr interval.

309

310 **4 Discussion**

311 Our objective with this manuscript was to generate the simplest reasonable model to predict CO₂ from the LR04
312 $\delta^{18}\text{O}$ benthic stack and to test the predictions against available observations. It is possible that the fit between
313 observed and our predicted CO₂ data could be further improved using a non-linear approach. However, we
314 refrain from a non-linear approach for several key reasons. First, a scatter plot of the LR04 $\delta^{18}\text{O}$ benthic stack
315 versus observed ice core CO₂ over the past 800 kyr yields a Pearson's correlation coefficient (R) of -0.82 (Fig.
316 2), indicating that $\sim 68\%$ of the variance in observed CO₂ is shared with the benthic stack. This is similar to that
317 reported in ordinary linear least-squares regression ($R^2=0.70$) by Berends *et al.* (2021b). Importantly, there is no
318 evidence in this scatter plot for departure from the linear relationship at high or low CO₂ or benthic $\delta^{18}\text{O}$ levels.
319 Second, following the approach of Chalk *et al.*, 2017 and interpreting the upper 25th percentile of CO₂ data as
320 representing mean interglacial stage CO₂ and the lower 25th percentile of CO₂ data as representing mean glacial
321 stages CO₂ levels, we see that our predicted interglacial mean value for the past 800 kyr ($253.1 \pm 2.3 \text{ ppm}$)
322 closely overlaps with the observed interglacial mean value ($253.9 \pm 4.1 \text{ ppm}$) and similarly, the predicted glacial
323 stage mean ($199.7 \pm 1.7 \text{ ppm}$) closely overlaps with the observed glacial stage mean ($202.0 \pm 3.2 \text{ ppm}$). Third,
324 the predictions are remarkably insensitive to bootstrap analysis in which 50 % of that data are omitted with each
325 iteration of the GLS model. Such insensitivity to the bootstrap analysis and accurate prediction of glacial and
326 interglacial state CO₂ values would be unlikely in the case of major non-linear dependencies between the LR04
327 predictor and CO₂ response variables. Fourth, non-linear approaches would risk generating an improved fit due
328 to statistical artefacts that do not meaningfully relate to any dependence between benthic $\delta^{18}\text{O}$ and CO₂. Finally,
329 the specific causes and sources and sinks involved in glacial to interglacial and millennial-scale CO₂ variations

330 remain poorly constrained (e.g. Archer *et al.*, 2000; Sigman *et al.*, 2010; Gottschalk *et al.*, 2019). Given this
331 process-uncertainty, the GLS model fits our criteria of the simplest reasonable model. Further, the use of benthic
332 $\delta^{18}\text{O}$ to predict atmospheric CO_2 has precedence; in response to the EPICA challenge (Wolff *et al.*, 2004) N.
333 Shackleton predicted atmospheric CO_2 out to 800 kyr, based on a number of benthic $\delta^{18}\text{O}$ records from the East
334 Pacific (Wolff, 2005).

335

336 There are several caveats with blue ice data that may affect its use to evaluate our GLS model predictions. The
337 blue ice data may have been subject to diffusional smoothing of CO_2 (e.g. Yan *et al.*, 2019), which would act in
338 the direction of elevating the (lower 25th percentile) assumed glacial concentrations above the glacial
339 atmospheric values and reducing the (upper 25th percentile) assumed interglacial concentrations. There is also
340 the potential for artificially elevated CO_2 concentrations in blue ice due in-situ respiration of CO_2 due to
341 microbial activity in detrital matter. Respiration effects are screened for by measurements of $\delta^{13}\text{C}$ of CO_2 ,
342 however it is difficult to demonstrate that all samples are unaffected (Yan *et al.*, 2019). These uncertainties
343 support our argument that the GLS-model predictions are not rejected by the available observed BI- CO_2 data.

344

345 We consider the BI- CO_2 data to provide the most reliable measurements of CO_2 concentration, in the absence of
346 a continuous ice core record across the MPT. However, further comparison of our CO_2 predictions can also be
347 made against CO_2 proxy data from non-ice core archives (Fig 4A). We consider here $\delta^{11}\text{B}$ -based atmospheric
348 CO_2 reconstructions (Chalk *et al.*, 2017, Dyez *et al.* 2018 and Guillermic *et al.* 2022) and a recent atmospheric
349 CO_2 reconstruction from $\delta^{13}\text{C}$ of leaf wax (Yamamoto *et al.*, 2022). The continuous $\delta^{11}\text{B}$ -based reconstructions
350 of Dyez *et al.*, (2018) overlap PRED- CO_2 from $\sim 1.38 - 1.5$ Mya while the Chalk *et al.*, (2017) reconstruction
351 overlaps PRED- CO_2 from 1.09 – 1.43 Mya. Discrete reconstructions from Guillermic *et al.* (2022) are
352 distributed non-uniformly across the ~ 800 to 1.5 Mya interval. For the two continuous $\delta^{11}\text{B}$ -based
353 reconstructions (Chalk *et al.*, (2017) and Dyez *et al.*, (2018)) the glacial CO_2 levels appear consistent with the
354 PRED- CO_2 record, within their reported 30 – 60 ppm uncertainties. However, $\delta^{11}\text{B}$ -based interglacial stages in
355 these reconstructions exceed those of the PRED- CO_2 record (Fig. 4A). The Guillermic *et al.* (2022)
356 reconstructions suggest a larger range of CO_2 concentrations than the overlapping intervals of PRED- CO_2 and of
357 the two continuous $\delta^{11}\text{B}$ -based reconstructions (Fig. 4A). The large range of the Guillermic *et al.* (2022) data
358 and the high interglacial maxima in the Chalk *et al.* (2017) and Dyez *et al.*, (2018) data, all significantly exceed
359 the range and interglacial maxima from the BI- CO_2 estimates. These discrepancies internally between different
360 $\delta^{11}\text{B}$ -based CO_2 reconstructions and between the $\delta^{11}\text{B}$ -based reconstructions and the BI- CO_2 data, may be due to
361 uncertainties associated with the $\delta^{11}\text{B}$ proxy transfer function. The $\delta^{11}\text{B}$ -based CO_2 reconstructions are
362 dependent on assumptions about multiple components of the carbonate system, including local marine carbon
363 chemistry and the CO_2 saturation state in the past (Hönisch *et al.*, 2009). Evidence that $\delta^{11}\text{B}$ -based
364 reconstructions may overestimate interglacial stage CO_2 is also seen in data from Chalk *et al.*, (2017) spanning
365 ca. 0–250 kya, where the $\delta^{11}\text{B}$ -based interglacial CO_2 levels exceed the continuous ice core CO_2 record by up to
366 ca. 30 ppm.

367

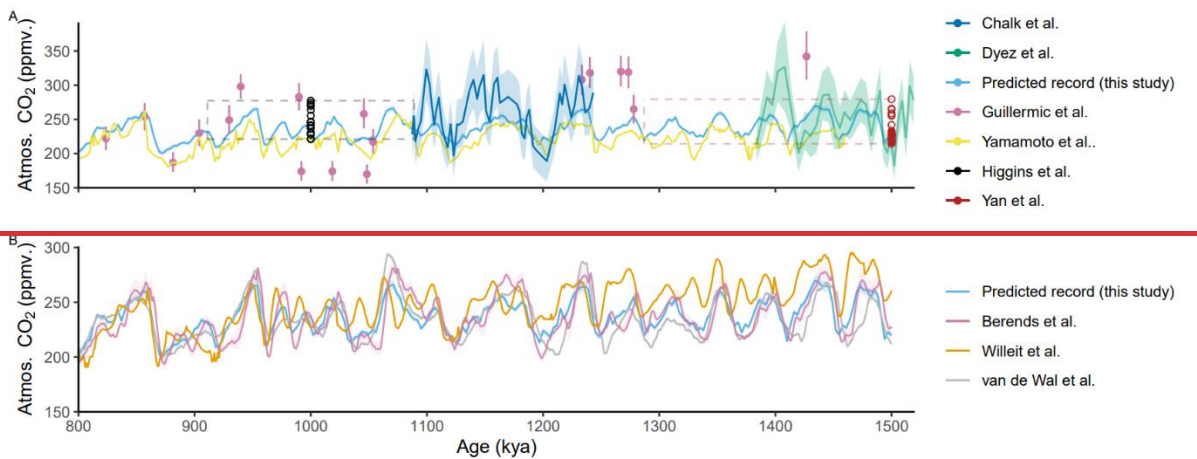
368 By comparison, the $\delta^{13}\text{C}$ of leaf wax data (Yamamoto *et al.*, 2022) has a similar glacial to interglacial range as
369 PRED- CO_2 , but a ca. 20ppm lower mean concentration than our predictions (Fig 4A). Hence, our PRED- CO_2

370 data fall lower than interglacial $\delta^{11}\text{B}$ -based interglacial levels but are higher than the $\delta^{13}\text{C}$ of leaf-wax based
 371 estimate. The strong spread between these different proxies and the large associated uncertainty of the
 372 alternative marine and leaf wax proxy- CO_2 reconstructions mean that we do not find cause from the existing
 373 CO_2 proxy data to reject our predictions nor our associated null-hypothesis.

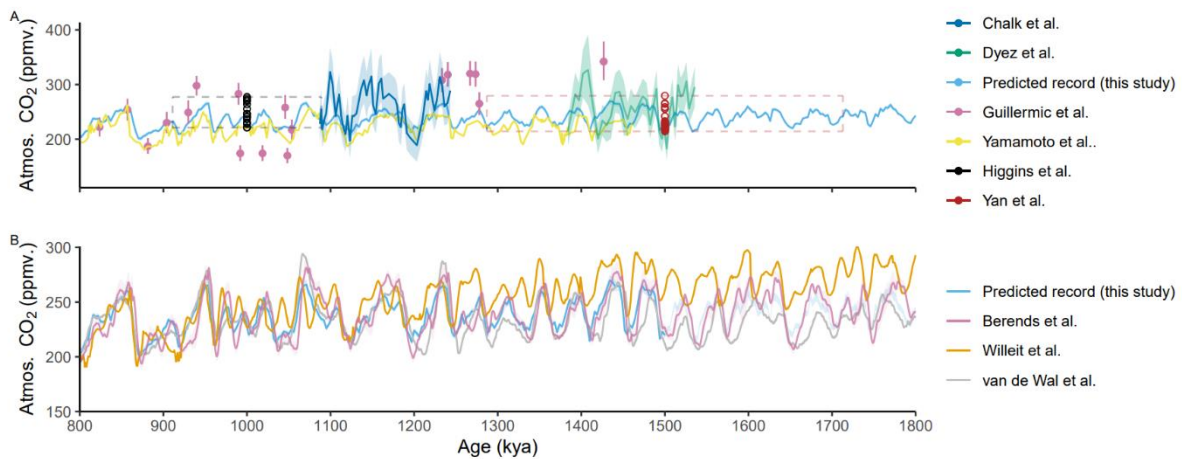
374

375 We also compare our predictions to existing more complex model simulations (Fig 4B.). First, against a
 376 transient simulation using an intermediate-complexity earth system model (CLIMBER-2) by Willeit *et al.*
 377 (2019). This study suggests a combination of gradual regolith removal and atmospheric CO_2 decline can explain
 378 the long-term climate variability over the past 3 Myr. Second, against a longer-term reconstruction by van de
 379 Wal *et al.* (2011), which uses benthic $\delta^{18}\text{O}$ that utilises deep-sea benthic isotope records to reconstruct a
 380 continuous CO_2 record over the past 20 Myr. Third, a CO_2 reconstruction based on an inverse forward-
 381 modelling approach forced by the LR04 benthic stack, in which the forward model is incrementally updated
 382 through interaction with general circulation model snapshots and the ANICE 3-D ice-sheet-shelf model
 383 (Berends *et al.* 2021b). Our simple GLS model demonstrates a similar long-term trend and timing of glacial-
 384 interglacial signals and an atmospheric CO_2 level that sits approximately mid-way between the van de Wal *et al.*
 385 (2011), and Willeit *et al.* (2019) models and is remarkably similar to the Berends *et al.* (2021b) reconstruction,
 386 despite their different approach. Notably the Berends *et al.* reconstruction shows greater glacial to interglacial
 387 amplitude in the CO_2 signal compared to our GLS-model. The decreasing linear trend in CO_2 in Willeit *et al.*
 388 (2019), which is not seen in the other reconstructions, was directly prescribed in that study to induce Northern
 389 Hemisphere glaciation at 2.6 Myr ago.

390



391



392

393 **Figure 4: A) Predicted CO₂ (this work) compared to observed, proxy CO₂ estimates from a range of other**
 394 **sources: $\delta^{11}\text{B}$ -based pCO₂ reconstructions and measurements by Dyez *et al.* (2018), Guillermic *et al.***
 395 **(2022); Chalk *et al.*, (2017); blue ice CO₂ measurements by Yan *et al.* (2019) and Higgins *et al.* (2015);**
 396 **$\delta^{13}\text{C}$ leaf wax proxy reconstructions by Yamamoto *et al.* (2022). The dashed boxes indicate the dating**
 397 **uncertainty and range of the respective BI-CO₂ records. B) Our predicted record compared to various**
 398 **model simulations: a regolith removal hypothesis simulation by Willeit *et al.* (2019); and inverse-model**
 399 **based CO₂ reconstructions by van de Wal *et al.* (2011), and Berends *et al.*, (2021b).**

400

401 A complete and critical test of our and other CO₂ predictions awaits the upcoming analysis of the continuous
 402 oldest ice core records. We now discuss some potential applications of the PRED-CO₂ record for hypothesis
 403 testing on the cause of the MPT.

404

405 PRED-CO₂ shows a long-term decline in glacial CO₂ across the MPT, but no long-term decrease in interglacial
 406 CO₂. This pattern is consistent with the boron-isotope-based CO₂ reconstructions shown earlier, where it is often
 407 described as an increase in the interglacial to glacial CO₂ difference (e.g., Chalk *et al.*, 2017; Hönlisch *et al.*,
 408 2009). Chalk *et al.* (2017) concludes that the MPT was initiated by a change in ice sheet dynamics and that
 409 longer and higher-ice volume post-MPT ice ages are sustained by carbon cycle feedbacks, in particular dust
 410 fertilisation of the Southern Ocean. **The fact that** our LR04-based prediction of CO₂ captures this same trend,
 411 **with predicted glacial CO₂ fairly constant from 1.5 to ca. 1.0 Mya before declining from 1.0 to 0.6 Mya, reflects**
 412 **that the LR04 benthic stack** also features an increase in the interglacial to glacial benthic $\delta^{18}\text{O}$ difference across
 413 this same interval, which is dominated by the glacial stage changes (Fig 3A.). Here, a comparison of PRED-CO₂
 414 to a realised continuous oldest ice core record will be of value. The agreement or disagreement would inform on
 415 the proportionality of the CO₂ coupling with ice volume; if there were a major new or non-linear process across
 416 the MPT that changed the nature of coupling between CO₂ and ice volume the PRED-CO₂ and observed CO₂
 417 records would be expected to diverge.

418

419 Another avenue to use the PRED-CO₂ record for hypothesis testing on the cause of the MPT concerns the phase
 420 locking hypothesis. The phase locking hypothesis is proposed to explain the absence of precession-related (23
 421 kyr) periods in the LR04 benthic stack prior to the MPT (Fig 1), despite the strong precession cycle in insolation

422 (Raymo *et al.*, 2006, Morée *et al.*, 2021). The key concept is that prior to the MPT the Northern Hemisphere and
423 Antarctic ice sheets were responsive (in ice volume) to insolation changes in the precession band, but because
424 precession forcing is out of phase between the hemispheres, the ice volume changes were opposing between the
425 hemispheres and therefore cancelled in the benthic stack. This cancellation of the precession signal left
426 insolation forcing in the 41 kyr obliquity band to dominate globally integrated ice volume changes expressed in
427 the benthic stack. A transition from a smaller and more dynamic terrestrial-terminating Antarctic ice sheet to a
428 larger and more stable marine-terminating ice sheet with cooling climate across the MPT (e.g. Elderfield *et al.*,
429 2012) is then proposed to remove sensitivity of Antarctic ice volume to local precession forcing in favour of
430 quasi-100 kyr ice volume changes that are in phase between the hemispheres (Raymo *et al.*, 2006). ~~is then~~
431 ~~proposed to remove sensitivity of Antarctic ice volume to precession forcing and to suppress ice sheet~~
432 ~~sensitivity to the obliquity band in favour of quasi-100kyr ice volume changes that are in phase between the~~
433 ~~hemispheres (Raymo *et al.*, 2006).~~

434

435 Recently presented data from Yan *et al.* (2022), lend some support to the phase locking hypothesis, specifically
436 with evidence that pre-MPT Antarctic temperature (and by extension ice volume) is positively correlated with a
437 local precession-band insolation proxy based on the oxygen to nitrogen ratio of trapped air (Yan *et al.*, 2022).
438 Whereas the correlation becomes negative in the blue ice and continuous ice core data in the post-MPT record.
439 If Yan *et al.*, (2022) is correct and the phase locking hypothesis holds, then an implication is that prior to the
440 MPT, Antarctic climate, Antarctic ice volume and by extension Southern Ocean climate conditions, would fall
441 out of phase with the LR04 benthic stack. To now extend the argument to potential impacts on CO₂ exchange, if
442 the phase locking hypothesis holds, then prior to the MPT the Antarctic and Southern Ocean climate conditions
443 and by extension the Southern Ocean mechanisms of CO₂ exchange described earlier, would also be expected to
444 fall out of phase with the benthic stack. Since our regression model assumes continuation of the in-phase
445 relationship between the benthic stack and Antarctic and Southern Ocean climate conditions (as inherited from
446 the post-MPT training data) we would expect to see major disagreement between our pre-MPT CO₂ predictions
447 and a realised oldest ice continuous ice core CO₂ record.

448

449 **5 Summary and Conclusions**

450 In this study we have used a simple generalised least squares (GLS) model to predict atmospheric CO₂ from the
451 LR04 benthic $\delta^{18}\text{O}$ stack for the period spanning the mid-Pleistocene transition, 800–1800 kyr. Our CO₂
452 prediction is therefore based on the assumption that the physical processes linking CO₂, sea level, global ice
453 volume and ocean temperature over the past 800 kyr do not fundamentally change across the 800–1800 kya time
454 period. The null-hypothesis is deliberately simplistic on the basis that differences between our predictions and
455 observed or proxy CO₂ records may be revealing of the physical processes involved in the mid-Pleistocene
456 Transition.

457

458 We made initial tests of the null hypothesis by comparing our predicted CO₂ record to existing discrete blue ice
459 CO₂ records and other non-ice-core proxy-CO₂ records from the 800–1800 kyr interval. Our predicted CO₂
460 concentrations do not show any systematic departure from observed blue ice CO₂ concentrations. The
461 predictions are marginally lower (during glacial *and* interglacial stages) than those observed in blue ice from

462 1000 ± 89 kya and marginally higher than observed in blue ice data from 1.5 Mya ± 213 kyr. Our predictions
463 were generally lower than interglacial $\delta^{11}\text{B}$ -based- CO_2 reconstructions, but higher than recent $\delta^{13}\text{C}$ of leaf-wax
464 based CO_2 reconstructions. Overall, we do not find clear evidence from the existing blue ice or proxy CO_2 data
465 to reject our predictions nor our associated null-hypothesis. The definitive test of our and other CO_2 predictions
466 therefore awaits the future analysis of the upcoming continuous oldest ice core records. The PRED- CO_2 record
467 presented here should provide a useful comparison to forthcoming oldest ice core records and opportunity to
468 provide further constraints on the processes involved in the MPT.

469

470 **Author contributions**

471 Project design by JBP, TRV and JRWM and supervision by TRV and JBP. Data analysis and figures by JRWM
472 with input from all authors. Writing led by JRMV and JBP. All authors contributed to and agreed on the final
473 version of the manuscript.

474

475 **Competing interests**

476 The authors declare that they have no competing interests.

477

478 **Disclaimer**

479 This study, to the best of the author(s) knowledge and belief, contains no material previously published or
480 written by another person, except where due reference is made in the text of the study.

481

482 **Acknowledgements**

483 We acknowledge assistance from Simon Wotherspoon (Institute for Marine and Antarctic Studies) in
484 appropriate model selection methods. [We thank Lorraine Lisiecki and Constantijn Berends's for their](#)
485 [constructive reviews, which greatly improved the manuscript](#) This research was supported by the Australian
486 Government through Australian Antarctic Science projects 4632, the Million Year Ice Core (MYIC) Project and
487 by the Australian Government Department of Industry Science Energy and Resources, grant ASCI000002.

488

489 **Data availability**

490 The PRED- CO_2 data presented here will be publicly archived at the Australian Antarctic Data Centre
491 (https://data.aad.gov.au/metadata/AAS_4632_Martin_etal_CP_2024<https://data.aad.gov.au/>[full link provided](#)
492 [upon publication](#)<<=>).

493

494 **References**

- 495 Archer, D., Winguth, A., D. Lea, and Mahowald, N.: What caused the glacial/interglacial atmospheric
496 pCO_2 cycle?, *Rev. Geophys.*, 38, 159–189, 2000, <https://doi.org/10.1029/1999RG000066>, 2000.
497
498 Bazin, L., Landais, A., Lemieux-Dudon, B., Toyé Mahamadou Kele, H., Veres, D., Parrenin, F., Martinerie, P.,
499 Ritz, C., Capron, E., Lipenkov, V., Loutre, M.-F., Raynaud, D., Vinther, B., Svensson, A., Rasmussen, S.,
500 Severi, M., Blunier, T., Leuenberger, M., Fischer, H., Masson-Delmotte, V., Chappellaz, J., and Wolff, E.: An
501 optimized multi-proxies, multi-site Antarctic ice and gas orbital chronology (AICC2012): 120-800 ka, *Clim.*
502 *Past*, 9, 1715-1731, <https://doi.org/10.5194/cp-9-1715-2013>, 2013.
503

504 Bereiter, B., Eggleston, S., Schmitt, J., Nehrbass-Ahles, C., Stocker, T. F., Fischer, H., Kipfstuhl, S., and
505 Chappellaz, J.: Revision of the EPICA Dome C CO₂ record from 800 to 600 ky before present, *Geophys. Res.*
506 *Let.*, 42, 542-549, <https://doi.org/10.1002/2014gl061957>, 2015.

507

508 Berends, C. J., Köhler, P., Lourens, L. J., and van de Wal, R. S. W.: On the cause of the mid-Pleistocene
509 transition., *Rev. Geophys.*, 59, e2020RG000727. <https://doi.org/10.1029/2020RG000727>, 2021a.

510

511 Berends, C. J., de Boer, B., and van de Wal, R. S. W.: Reconstructing the evolution of ice sheets, sea level, and
512 atmospheric CO₂ during the past 3.6 million years. *Clim. Past*, 17, 361–377, [http://doi.org/10.5194/cp-17-361-](http://doi.org/10.5194/cp-17-361-2021)
513 2021, 2021b.

514

515 Berger, A., Li, X. S., and Loutre, M. F.: Modelling northern hemisphere ice volume over the last 3Ma,
516 *Quaternary. Sci. Rev.*, 18, 1-11, [https://doi.org/10.1016/S0277-3791\(98\)00033-X](https://doi.org/10.1016/S0277-3791(98)00033-X), 1999.

517

518 Broecker, W.S.: Glacial to interglacial changes in ocean chemistry, *Prog. Oceanogr.*, 11 (2), 151-197.
519 [https://doi.org/10.1016/0079-6611\(82\)90007-6](https://doi.org/10.1016/0079-6611(82)90007-6), 1982.

520

521 Chalk, T., Hain, M., Foster, G., Rohling, E., Sexton, P., Badger, M., Cherry, S., Hasenfratz, A., Haug, G.,
522 Jaccard, S., Martínez-García, A., Pälike, H., Pancost, R., and Wilson, P.: Causes of ice age intensification across
523 the Mid-Pleistocene Transition, *P. Natl. Acad. Sci. USA.*, 114, 13114-13119,
524 <https://doi.org/10.1073/pnas.1702143114>, 2017.

525

526 Clark, P. U., Archer, D., Pollard, D., Blum, J. D., Rial, J. A., Brovkin, V., Mix, A. C., Pisias, N. G., and Roy,
527 M.: The middle Pleistocene transition: characteristics, mechanisms, and implications for long-term changes in
528 atmospheric pCO₂, *Quat. Sci. Rev.*, 25, 3150-3184, <https://doi.org/10.1016/j.quascirev.2006.07.008>, 2006.

529

530 Clark, P. U. and Pollard, D.: Origin of the Middle Pleistocene Transition by ice sheet erosion of regolith,
531 *Paleoceanography*, 13, 1-9, <https://doi.org/10.1029/97pa02660>, 1998.

532

533 Dyez, K.A., Hönisch, B., and Schmidt, G.A.: Early Pleistocene obliquity-scale pCO₂ variability at ~1.5 million
534 years ago. *Paleoceanogr. Paleoclimatol.*, 33, no. 11, 1270-1291, <https://doi.org/10.1029/2018PA003349>, 2018.

535

536 Elderfield, H., Ferretti, P., Greaves, S., Crowhurst, S., McCave, N., and Piotrowski, A.M.: Evolution of Ocean
537 Temperature and Ice Volume Through the Mid-Pleistocene Climate Transition, *Science*, 337,704-709,
538 <https://doi.org/10.1126/science.1221294>, 2012.

539

540 Gottschalk, J., Battaglia, G., Fischer, H., Frölicher, T.L., Jaccard, S.L., Jeltsch-Thömmes, A., Joos, F., Köhler,
541 P., Meissner, K.J., Menviel, L., Nehrbass-Ahles, C., Schmitt, J., Schmittner, A., Skinner, L.C., and Stocker,
542 T.G.: Mechanisms of millennial-scale atmospheric CO₂ change in numerical model simulations, *Quaternary.*
543 *Sci. Rev.*, 220, 30-74, <https://doi.org/10.1016/j.quascirev.2019.05.013>, 2019.

544

545 Guillermic, M., Misra, S., Eagle, R., and Tripathi, A.: Atmospheric CO₂ estimates for the Miocene to Pleistocene
546 based on foraminiferal $\delta^{11}\text{B}$ at Ocean Drilling Program Sites 806 and 807 in the Western Equatorial Pacific,
547 *Clim. Past*, 18(2), 183-207, <https://doi.org/10.5194/cp-18-183-2022>, 2022.

548

549 Hasenfratz, A. P., Jaccard, S. L., Martínez-García, A., Sigman, D. M., Hodell, D. A., Vance, D., Bernasconi, S.
550 M., Kleiven, H. F., Haumann, F. A., and Haug, G. H.: The residence time of Southern Ocean surface waters and
551 the 100,000-year ice age cycle, *Science*, 363, 1080, <https://doi.org/10.1126/science.aat7067>, 2019.

552

553 Higgins, J. A., Kurbatov, A. V., Spaulding, N. E., Brook, E., Introne, D. S., Chimiak, L. M., Yan, Y.,
554 Mayewski, P. A., and Bender, M. L.: Atmospheric composition 1 million years ago from blue ice in the Allan
555 Hills, Antarctica, *P. Natl. Acad. Sci. USA.*, 112, 6887, <https://doi.org/10.1073/pnas.1420232112>, 2015.

556

557 Hönisch, B., Hemming, N. G., Archer, D., Siddall, M., and McManus, J. F.: Atmospheric Carbon Dioxide
558 Concentration Across the Mid-Pleistocene Transition, *Science*, 324, 1551,
559 <https://doi.org/10.1126/science.1171477>, 2009.

560

561 Huybers, P., & Wunsch, C. (2005). Obliquity pacing of the late Pleistocene glacial terminations. *Nature*,
562 434(7032), 491-494.

563

564 International Panel on Climate Change: Climate change 2001; IPCC third assessment report, IPCC, Geneva,
565 2001.
566

567 International Partnerships in Ice Core Sciences: The oldest ice core: A 1.5 million year record of climate and
568 greenhouse gases from Antarctica [White paper]. [https://igbp-](https://igbp-scor.pages.unibe.ch/sites/default/files/download/docs/working_groups/ipics/white-papers/ipics_oldaa_final.pdf)
569 [scor.pages.unibe.ch/sites/default/files/download/docs/working_groups/ipics/white-papers/ipics_oldaa_final.pdf](https://igbp-scor.pages.unibe.ch/sites/default/files/download/docs/working_groups/ipics/white-papers/ipics_oldaa_final.pdf),
570 accessed 06/12/2023, 2020.
571

572 Jouzel, J., Masson-Delmotte, V., Cattani, O., Dreyfus, G., Falourd, S., Hoffmann, G., Minster, B., Nouet, J.,
573 Barnola, J. M., Chappellaz, J., Fischer, H., Gallet, J. C., Johnsen, S., Leuenberger, M., Loulergue, L., Luethi, D.,
574 Oerter, H., Parrenin, F., Raisbeck, G., Raynaud, D., Schilt, A., Schwander, J., Selmo, E., Souchez, R., Spahni,
575 R., Stauffer, B., Steffensen, J. P., Stenni, B., Stocker, T. F., Tison, J. L., Werner, M., and Wolff, E. W.: Orbital
576 and Millennial Antarctic Climate Variability over the Past 800,000 Years, *Science*, 317, 793,
577 <https://doi.org/10.1126/science.1141038>, 2007.
578

579 Lisiecki, L. E. and Raymo, M. E.: A Pliocene-Pleistocene stack of 57 globally distributed benthic $\delta^{18}\text{O}$ records,
580 *Paleoceanography*, 20, PA1003, <https://doi.org/10.1029/2004pa001071>, 2005.
581

582 Martínez-García, A., Sigman, D.M., Ren, H., Anderson, R.F., Straub, M., Hodell, D.A., Jaccard, S.L., Eglinton,
583 T.I., and Haug, G.H.: Iron fertilization of the subantarctic ocean during the last ice age, *Science*, 343 (6177),
584 1347-1350, <https://doi.org/10.1126/science.1246848>, 2014.
585

586 McClymont, E.L., Sostdian, S.M., and Rosell-Melé, A.: Pleistocene sea-surface temperature evolution: Early
587 cooling, delayed glacial intensification, and implications for the mid-Pleistocene transition. *Earth. Sci. Rev.*,
588 123, 173-193, <https://doi.org/10.1016/j.earscirev.2013.04.006>, 2013.
589

590 Millero, F. J.: Thermodynamics of the carbon dioxide system in the oceans, *Geochim. Cosmochim. Acta.*, 59,
591 661-677, [https://doi.org/10.1016/0016-7037\(94\)00354-O](https://doi.org/10.1016/0016-7037(94)00354-O), 1995.
592

593 Morée, A. L., Sun, T., Bretones, A., Straume, E. O., Nisancioglu, K., and Gebbie, G.: Cancellation of the
594 precessional cycle in $\delta^{18}\text{O}$ records during the Early Pleistocene. *Geophys. Res. Lett.*, 48,
595 e2020GL090035. <https://doi.org/10.1029/2020GL090035>, 2021.
596

597 Petit, J. R., Jouzel, J., Raynaud, D., Barkov, N. I., Barnola, J. M., Basile, I., Bender, M., Chappellaz, J., Davis,
598 M., Delaygue, G., Delmotte, M., Kotlyakov, V. M., Legrand, M., Lipenkov, V. Y., Lorius, C., Pépin, L., Ritz,
599 C., Saltzman, E., and Stievenard, M.: Climate and atmospheric history of the past 420,000 years from the
600 Vostok ice core, Antarctica, *Nature*, 399, 429-436, <https://doi.org/10.1038/20859>, 1999.
601

602 Raymo, M., Lisiecki, L., and Nisancioglu, K.: Plio-Pleistocene Ice Volume, Antarctic Climate, and the Global
603 18O Record, *Science*, 313, 492-495, <https://doi.org/10.1126/science.1123296>, 2006.
604

605 Raymo, M., Ruddiman, W., and Froelich, P.: Influence of Late Cenozoic mountain building on ocean
606 geochemical cycles, *Geology*, 16, 649-653, [https://doi.org/10.1130/0091-](https://doi.org/10.1130/0091-7613(1988)016<0649:IOLCMB>2.3.CO;2)
607 [7613\(1988\)016<0649:IOLCMB>2.3.CO;2](https://doi.org/10.1130/0091-7613(1988)016<0649:IOLCMB>2.3.CO;2), 1988.
608

609 Raymo, M. E.: The timing of major climate terminations, *Paleoceanography*, 12, 577-585,
610 <https://doi.org/10.1029/97PA01169>, 1997.
611

612 [Raymo, M. E. and Huybers, P.: Unlocking the mysteries of the ice ages, *Nature*, 451, 284-285,](https://doi.org/10.1038/nature06589)
613 <https://doi.org/10.1038/nature06589>, 2008.
614

615 Röthlisberger, R., Bigler, M., Wolff, E. W., Joos, F., Monnin, E., and Hutterli, M. A.: Ice core evidence for the
616 extent of past atmospheric CO_2 change due to iron fertilisation, *Geophys. Res. Lett.*, 31, L16207,
617 <https://doi.org/10.1029/12004GL020338>, 2004.
618

619 Ruddiman, W. F., Raymo, M. E., Martinson, D. G., Clement, B. M., and Backman, J.: Pleistocene evolution:
620 Northern hemisphere ice sheets and North Atlantic Ocean, *Paleoceanography*, 4, 353-412,
621 <https://doi.org/10.1029/PA004i004p00353>, 1989.
622

623 Shackleton, N. J. and Pisias, N. G.: Atmospheric Carbon Dioxide, Orbital Forcing, and Climate. In: *The Carbon*
624 *Cycle and Atmospheric CO₂: Natural Variations Archean to Present*, <https://doi.org/10.1029/GM032p0303>,
625 1985.

626

627 Shugi, H., The older the ice, the better the science. *Adv. Polar Sci.*, 23, 121-122,
628 <https://doi.org/10.13679/j.advps.2022.0004>, 2022.

629

630 Stephens, B.B., Keeling, R.F.: The influence of Antarctic sea ice on glacial–interglacial CO₂ variations. *Nature*,
631 404, 171–174, <https://doi.org/10.1038/35004556>, 2000.

632

633 Tzedakis, P. C., Crucifix, M., Mitsui, T., and Wolff, E. W.: A simple rule to determine which insolation cycles
634 lead to interglacials, *Nature*, 542, 427–432, <https://doi.org/10.1038/nature21364>, 2017.

635

636 Ushie, H., and Matsumoto, K.: The role of shelf nutrients on glacial-interglacial CO₂: A negative
637 feedback, *Global Biogeochem. Cy.*, 26, GB2039, <https://doi.org/10.1029/2011GB004147>., 2012.

638

639 van de Wal, R. S. W., de Boer, B., Lourens, L. J., Köhler, P., and Bintanja, R.: Reconstruction of a continuous
640 high-resolution CO₂ record over the past 20 million years. *Clim. Past*, 7, 1459–1469. [https://doi.org/10.5194/cp-](https://doi.org/10.5194/cp-7-1459-2011)
641 [7-1459-2011](https://doi.org/10.5194/cp-7-1459-2011), 2011.

642

643 Veres, D., Bazin, L., Landais, A., Toyé Mahamadou Kele, H., Lemieux-Dudon, B., Parrenin, F., Martinerie, P.,
644 Blayo, E., Blunier, T., Capron, E., Chappellaz, J., Rasmussen, S., Severi, M., Svensson, A., Vinther, B., and
645 Wolff, E.: The Antarctic ice core chronology (AICC2012): an optimized multi-parameter and multi-site dating
646 approach for the last 120 thousand years, *Clim. Past*, 9, 1733–1748, <https://doi.org/10.5194/cp-9-1733-2013>,
647 2013.

648

649 Willeit, M., Ganopolski, A., Calov, R., and Brovkin, V.: Mid-Pleistocene transition in glacial cycles explained by
650 declining CO₂ and regolith removal, *Sci. Adv.*, 5, eaav7337, doi: 10.1126/sciadv.aav7337, 2019.

651

652 Wolff, E. W., Chappella, J., Fischer, H., Kull, C., Miller, H., Stocker, T. F., and Watson, A. J.: The EPICA
653 challenge to the Earth system modeling community, *EOS*, 85, 363363, <https://doi.org/10.1029/2004EO380003>,
654 2004.

655

656 Wolff, E. W., Kull, C., Chappellaz, J., Fischer, H., Miller, H., Stocker, T. F., Watson, A. J., Flower, B., Joos, F.,
657 Köhler, P., Matsumoto, K., Monnin, E., Mudelsee, M., Paillard, D., and Shackleton, N.: Modeling past
658 atmospheric CO₂: results of a challenge, *EOS*, 86 (38), 341–345, <http://doi.org/10.1029/2005EO380003>, 2005.

659

660 Yamamoto, M., Clemens, S.C., Seki, O., Tsuchiya, Y., Huang, Y., O’ishi, R., and Abe-Ouchi, A.: Increased
661 interglacial atmospheric CO₂ levels followed the mid-Pleistocene Transition, *Nat. Geosci.*, 15(4), 307–313,
662 <https://doi.org/10.1038/s41561-022-00918-1>, 2022.

663

664 Yan, Y., Bender M.I., Brook, E.J., Clifford, H.M., Kemeny, P.C., Kurbatov, A.V., Mackay, S., Mayewski,
665 P.A., Ng, J., Severinghaus J.P., and Higgins, J.A.: Two-million-year-old snapshots of atmospheric gases from
666 Antarctic ice, *Nature*, 574(7780), 663–666, <https://doi.org/10.1038/s41586-019-1692-3>, 2019.

667

668 Yan, Y., Kurbatov, A.V., Mayewski, P.A., Shackleton, S., and Higgins, J.A.: Early Pleistocene East Antarctic
669 temperature in phase with local insolation. *Nat. Geosci.*, 16, 50–55, [https://doi.org/10.1038/s41561-022-01095-](https://doi.org/10.1038/s41561-022-01095-x)
670 [x](https://doi.org/10.1038/s41561-022-01095-x), 2022.